SLIDING-MODE CONTROL FOR LINEAR PERMANENT-MAGNET MOTOR POSITION TRACKING

Gerardo Tapia * **Arantxa Tapia** *

* *Systems Engineering & Control Department, University of the Basque Country, E.U.P.-D, Europa Plaza 1, 20018 Donostia-San Sebastián, Spain*

Abstract: Based on Utkin's research work regarding speed control of rotary motors, a position tracking algorithm for linear permanent magnet synchronous motors (LPMSM) is designed making use of multi-variable sliding-mode control and asymptotic observers. It is applicable to LPMSM's with either interior or surface-mounted magnets, no matter whether the armature is stationary or movable. Furthermore, the control signals yielded are able to drive the power transistors of the inverter feeding the motor directly, hence avoiding the employment of techniques such as PWM or SVM. Performance of the control structure proposed is evaluated on the simulation model of a commercially available LPMSM.

Keywords: Machining, linear motors, observers, permanent magnet motors, positioning systems, servo systems, sliding-mode control, synchronous machines.

1. INTRODUCTION

Applications entailing linear motors allow removing mechanical transmission elements, as magnetic fields transmit the required forces directly. As a result, higher speeds and accelerations, along with better precision at high speeds and reduction of noise levels and mechanical damages, can be achieved (Weidner and Quickel, 1999), (Renton and Elbestawi, 2001). In this context, there is currently a patent trend towards the employment of LPMSM's. This is mainly due to the fact that they present better dynamic performance and higher power density than their induction motor counterparts. But LPMSM's can also operate with larger air-gaps between the stationary and movable parts, which is a critical factor for several industrial sectors (Gieras and Piech, 2000).

On the other hand, position control schemes of linear motors are typically carried out by cascading fixed-gain PID-type controllers to vector (VC) or even direct thrust control (DTC) algorithms (Gieras and Piech, 2000), (Vas, 1998). Although satisfactory responses to step demands are provided, they do not perform so suitably in the general servo situation. In opposition, trajectory tracking is a major strength of the sliding-mode control approach adopted here (Utkin, 1993), (Utkin *et al.*, 1999) which, in addition to endowing the system with insensitivity to parameter variation, allows evading the use of PWM or SVM, just as DTC.

2. LPMSM MODELLING FOR CONTROLLER DESIGN

Roughly speaking, the physical structure of the LPMSM considered is composed of two main parts, as reflected in Fig. 1. The lower piece corresponds to the stationary element containing the

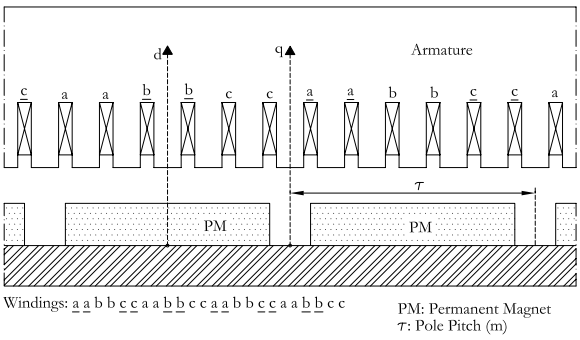

Fig. 1. Physical structure of the LPMSM

permanent magnets, while the upper component is the movable armature lodging the phase windings to be fed. Yet, it is not an unusual practice to place the permanent magnets and armature windings in the moveable and fixed parts, respectively. In any case, the air-gap between both elements allows the movement of the magnetic flux distribution travelling-wave, which interacts with the currents flowing through the armature windings to generate the driving force in the motion direction.

Even though different modelling approaches considering specific phenomena arising in linear motors —like edge effect— have been investigated, controller design is typically carried out based on models which are analogous to those devoted to rotary motors (Vas, 1996), (Vas, 1998). From this viewpoint, the state-space electromechanical model of a LPMSM, expressed according to the *d-q* reference frame fixed to the part lodging the permanent magnets —refer to Fig. 1—, may be given as follows (Gieras and Piech, 2000), (Boldea and Nasar, 2001)

$$di_d/dt = (v_d - R_s i_d + \omega_r L_q i_q)/L_d \quad (1)$$

$$di_q/dt = [v_q - R_s i_q - \omega_r (L_d i_d + \lambda_{PM})]/L_q \quad (2)$$

$$F_x = 1.5kP(\pi/\tau)[(L_d - L_q)\, i_d + \lambda_{PM}]i_q \quad (3)$$

$$du_s/dt = (F_x - F_{load} - f u_s)/M \quad (4)$$

$$dx/dt = u_s, \quad (5)$$

where i_d, i_q and v_d, v_q are the armature current and voltage direct- and quadrature-axis components, u_s and x represent the linear speed and position of the movable part, F_x and F_{load} correspond to the motor thrust and load force, and $\omega_r = k\,(\pi/\tau)\, u_s$. Constant k indicates whether the movable part is that containing the permanent magnets —$k = 1$— or the armature —$k = -1$. Parameters appearing in (1)–(4) are described in Table A.1 of Appendix A.

Clarke's 3-to-2 axes transformation allows expressing the armature voltage space-phasor, resulting from applying balanced v_a, v_b and v_c phase voltages, according to its natural *D-Q* reference frame —fixed to the armature— as:

$$v_D = (2v_a - v_b - v_c)/3 \quad (6)$$

$$v_Q = (v_b - v_c)/\sqrt{3}. \quad (7)$$

A further Park's transform, given by

$$v_d = v_D \cos\theta_r + v_Q \sin\theta_r \quad (8)$$

$$v_q = -v_D \sin\theta_r + v_Q \cos\theta_r, \quad (9)$$

where $\theta_r = k\,(\pi/\tau)\, x$, brings its components to the *d-q* reference frame. Furthermore, three-phase voltages v_a, v_b and v_c may be derived from the DC-link U_d voltage and the commutation state —provided by Boolean variables S_a, S_b and S_c— of the six power transistors which the inverter feeding the LPMSM armature is composed of (Vas, 1998); i.e.:

$$v_a = (2S_a - S_b - S_c)\, U_d/3 \quad (10)$$

$$v_b = (-S_a + 2S_b - S_c)\, U_d/3 \quad (11)$$

$$v_c = (-S_a - S_b + 2S_c)\, U_d/3. \quad (12)$$

Each armature phase is connected to the midpoint of one of the three inverter legs. $S_i = 1$; $i = a, b, c$, indicates that the upper transistor of the leg which armature phase 'i' is connected to is switched on, while its lower one remains switched off. Alternatively, $S_i = 0$ denotes that upper and lower transistors of leg 'i' are switched off and on, respectively.

3. SLIDING-MODE CONTROL ALGORITHM

The linear position tracking control algorithm presented throughout this section takes Utkin's research work concerning speed control of rotary motors as starting point (Utkin, 1993), (Utkin *et al.*, 1999). Specifically, it is designed by adopting his particular multi-variable approach to sliding-mode control, given that three voltages —v_a, v_b and v_c— need to be provided as control signals in order to feed the motor armature.

As controller design is accomplished by considering the general model in (1)–(5), it should be highlighted that the algorithm devised is valid regardless of which motor part is stationary and which movable —$k = 1$ or -1. Moreover, LPMSM's with both surface-mounted —$Ld = Lq$— or interior magnets —$L_d < L_q$— may be efficiently governed through the control system proposed next. In contrast, typical vector control schemes implemented on PMSM's turn out to be significantly different of one another, depending on whether magnets are surface-mounted or interior (Vas, 1998).

3.1 Synthesis of the control law

Three switching variables —s_1, s_2 and s_3— are defined so as to:

- Keep the motor linear position, x, on the desired trajectory.
- Govern the armature current i_d component so that, below the rated speed, the motor provides maximum thrust per current unit and, above it, field weakening operation is adopted to achieve maximum thrust per flux unit (Vas, 1998).
- Preserve a balanced three-phase voltage supply.

If, in addition to meeting these three requirements above, it is sought that time derivatives of s_1, s_2 and s_3 depend explicitly upon control inputs v_a, v_b and v_c, the following switching variables may be considered

$$\begin{aligned} s_1 = {} & \ddot{x}_0 - \ddot{x}\,(t) + 2\xi\omega_n\left[\dot{x}_0 - \dot{x}\,(t)\right] + \\ & + \omega_n^2\left[x_0 - x\,(t)\right] = \dot{u}_{s0} - \dot{u}_s\,(t) + \\ & + 2\xi\omega_n\left[u_{s0} - u_s\,(t)\right] + \omega_n^2\left[x_0 - x\,(t)\right] \end{aligned} \tag{13}$$

$$s_2 = i_{d0} - i_d\,(t) \tag{14}$$

$$s_3 = \int_0^t (v_a + v_b + v_c)\,dt, \tag{15}$$

where x_0 and u_{s0} represent the desired instantaneous linear position and speed, i_{d0} is the reference value for armature current component i_d, and ξ and ω_n correspond to the damping factor and natural frequency of the linear position error dynamics while vanishing in sliding regime —s_1=0.

Accordingly, if s_1, s_2 and s_3 were all kept equal to zero all the way through, both the linear position and i_d current component would be steered to their corresponding desired values, by feeding the LPMSM armature with balanced three-phase voltages. As a consequence, the objective may thus be viewed as keeping the whole system operating in the intersection of sliding surfaces s_1=0, $s_2 = 0$ and $s_3 = 0$. This implies that the design task is reduced to enforcing the sliding regime in the manifold $\mathbf{s} = \left[\, s_1 \;\; s_2 \;\; s_3 \,\right]^T = \mathbf{0}$, for the system given by (1)–(5), whose control input is $\mathbf{v} = \left[\, v_a \;\; v_b \;\; v_c \,\right]^T$.

Taking the time derivative on both sides of (13)–(15) and making use of expressions (1)–(9), the LPMSM dynamics may be transferred to subspace $\mathbf{s}$ to yield

$$\dot{\mathbf{s}} = \mathbf{F} + \mathbf{B}\mathbf{v}, \tag{16}$$

where

$$\mathbf{F} = \begin{bmatrix} f_1\left(i_d, i_q, u_s, F_{load}, \dot{F}_{load}, u_{s0}, \dot{u}_{s0}, \ddot{u}_{s0}\right) \\ \dfrac{di_{d0}}{dt} + \dfrac{R_s}{L_d} i_d - \dfrac{L_q}{L_d}\omega_r i_q \\ 0 \end{bmatrix} \tag{17}$$

$$\mathbf{B} = \begin{bmatrix} b_a & b_b & b_c \\ -\dfrac{2}{3L_d}\cos\gamma_a & -\dfrac{2}{3L_d}\cos\gamma_b & -\dfrac{2}{3L_d}\cos\gamma_c \\ 1 & 1 & 1 \end{bmatrix}, \tag{18}$$

and

$$b_i = \frac{kP\pi}{M\tau}\left(X\sin\gamma_i - Y\cos\gamma_i\right);\;\; i = a, b, c \tag{19}$$

$$X = \frac{1}{L_q}\left[\left(L_d - L_q\right) i_d + \lambda_{PM}\right],\;\; Y = \frac{L_d - L_q}{L_d} i_q \tag{20}$$

$$\gamma_a = \theta_r,\;\; \gamma_b = \theta_r - 2\pi/3,\;\; \gamma_c = \theta_r + 2\pi/3. \tag{21}$$

Consequently, assuming that it is sought to implement a multi-variable discontinuous control law of the form

$$\mathbf{v} = -(U_d/2)\,\mathrm{sgn}(\mathbf{s}^*);\;\; \mathbf{s}^* = \left[\, s_1^* \;\; s_2^* \;\; s_3^* \,\right]^T = \mathbf{B}^T\mathbf{s}, \tag{22}$$

Lyapunov function

$$\upsilon = 0.5\mathbf{s}^T\mathbf{s} \tag{23}$$

allows determining the value of the DC-link voltage, U_d, required. In fact, taking the time derivative of (23) on the state trajectories of system (16), and replacing $\mathbf{v}$ with control law (22) produces

$$\dot{\upsilon} = \mathbf{s}^T \underbrace{\left(\mathbf{F} + \mathbf{B}\mathbf{v}\right)}_{\dot{\mathbf{s}}} = \left(\mathbf{s}^*\right)^T \mathbf{F}^* - (U_d/2)\left|\mathbf{s}^*\right|, \tag{24}$$

where

$$\mathbf{F}^* = \left[\, f_1^* \;\; f_2^* \;\; f_3^* \,\right]^T = \mathbf{B}^{-1}\mathbf{F} \tag{25}$$

$$\left|\mathbf{s}^*\right| = \left|s_1^*\right| + \left|s_2^*\right| + \left|s_3^*\right|. \tag{26}$$

Examination of expressions (24)–(26) leads to conclude that fulfilment of the conditions given next

$$U_d > 2\left|f_i^*\right|;\;\; i = 1, 2, 3 \tag{27}$$

guarantees negativeness of $\dot{\upsilon}$. In other words, the origin of subspace $\mathbf{s}$ is asymptotically stable and the sliding regime arises in $\mathbf{s} = \mathbf{0}$, provided that DC-link voltage U_d is selected so that (27) is satisfied despite parameter variations and uncertainty in f_i^*; $i = 1, 2, 3$.

In practice, control law (22) can be realized just by driving the power transistors of the three inverter legs according to the following switching criterion:

$$S_{a,b,c} = \begin{cases} 1 & \text{if } s_{1,2,3}^* < 0 \\ 0 & \text{otherwise.} \end{cases} \tag{28}$$

3.2 Observer design

Implementation of control law (28) requires that linear position, speed and acceleration, as well

as armature current i_d and i_q components, are known. Assuming that both x and u_s are measured directly, the rest may be estimated by employing two different asymptotic observers. In addition to skipping the use of extra sensors, such observers allow by-passing control signal high-frequency components that may excite the unmodelled dynamics. Consequently, chattering associated to the latter may be evaded or, at least, reduced (Bondarev *et al.*, 1985).

Estimates $\hat{i}_d$ and $\hat{i}_q$ of armature current components are determined by the nonlinear observer expressed through state equations

$$d\hat{i}_d/dt = \Big(v_d - R_s\hat{i}_d + \omega_r L_q \hat{i}_q\Big)/L_d \tag{29}$$

$$d\hat{i}_q/dt = \Big[v_q - R_s\hat{i}_q - \omega_r\Big(L_d\hat{i}_d + \lambda_{PM}\Big)\Big]/L_q, \tag{30}$$

where voltage v_d and v_q components may be derived from the commutation state of the inverter power transistors —established by control law (28)— and the DC-link voltage, by following expressions (10)–(12) and (6)–(9).

Subtracting (1) and (2) from (29) and (30), respectively, the following state equations for estimation errors $\bar{i}_d = \hat{i}_d - i_d$ and $\bar{i}_q = \hat{i}_q - i_q$ arise:

$$d\bar{i}_d/dt = \left(-R_s\bar{i}_d + \omega_r L_q \bar{i}_q\right)/L_d \tag{31}$$

$$d\bar{i}_q/dt = \left(-R_s\bar{i}_q - \omega_r L_d \bar{i}_d\right)/L_q. \tag{32}$$

Now, taking the time derivative of Lyapunov function

$$\upsilon = 0.5\left(L_d\bar{i}_d^2 + L_q\bar{i}_q^2\right), \tag{33}$$

and bearing in mind that $L_d \leq L_q$, leads to

$$\dot{\upsilon} = -R_s\left(L_d\bar{i}_d^2 + L_q\bar{i}_q^2\right) \leq -\left(R_s/L_q\right)\upsilon, \tag{34}$$

which indicates that υ vanishes according to a decay rate of R_s/L_q —at least— and, as a result, $\hat{i}_d$ and $\hat{i}_q$ converge exponentially to their respective actual values.

As far as linear acceleration is concerned, it is estimated as

$$d\hat{u}_s/dt = \Big(\hat{F}_x - \hat{F}_L\Big)/M, \tag{35}$$

where F_L plays the same role of $F_{load} + fu_s$ in (4), and $\hat{F}_x$ is derived just by replacing i_d and i_q in (3) with their respective estimates; i.e.:

$$\hat{F}_x = 1.5kP\left(\pi/\tau\right)\Big[\left(L_d - L_q\right)\hat{i}_d + \lambda_{PM}\Big]\hat{i}_q. \tag{36}$$

On the other hand, $\hat{F}_L$ may be obtained by means of the Luenberger reduced order linear observer given next

$$d\hat{F}/dt = \left(\ell/M\right)\Big(-\hat{F} + \ell u_s + \hat{F}_x\Big), \tag{37}$$

where $\hat{F} = \hat{F}_L + \ell u_s$, and parameter ℓ is the observer gain. Considering that $\hat{F}_x$ is a satisfactory estimate of motor thrust —$\hat{F}_x \cong F_x$—, (37) may be rewritten as

$$d\hat{F}_L/dt + \ell\dot{u}_s = \left(\ell/M\right)\Big(-\hat{F}_L + M\dot{u}_s + F_L\Big). \tag{38}$$

Assuming that F_L varies slowly, $dF_L/dt \cong 0$, and (38) leads to

$$d\Big(\hat{F}_L - F_L\Big)/dt = -\left(\ell/M\right)\Big(\hat{F}_L - F_L\Big), \tag{39}$$

revealing that the desired convergence rate of $\hat{F}_L$ to F_L may be provided by proper choice of gain ℓ.

4. SIMULATION RESULTS

At this stage of the research work, the control structure presented throughout the previous section has only been tested via simulation. In any case, given that it is planned to check it experimentally over linear motor 1FN3 050-2WC00-0AA0 by SIEMENS at a later stage, the values of the parameters adopted for the LPMSM simulation model —collected in Table A.1 of Appendix A— correspond to those of such a motor. Moreover, Table A.2 shows the parameter values selected for both the controller and load force observer.

In an attempt to assess the controller performance under realistic conditions, both the load cycle and the tracking trajectory have been determined based on engineering example "Machining center with gantry axis," described in chapter 3 of (SIEMENS AG, 1999–2002). However, bearing in mind that the linear motor considered in such an example is considerably larger than 1FN3 050, the values of the total mass shifted, load force and maximum traversing speed have been adapted. Thereby, the peak and rms forces developed during a complete load cycle do not exceed the peak and nominal thrust values of linear motor 1FN3 050, respectively.

Both the desired and actual values —practically indistinguishable— of linear position and speed, as well as those of linear acceleration, are shown in Figs. 2(a), 2(b) and 3(a), respectively. The two latter evidence that the reference trajectory is composed of $2g$ acceleration, $-2g$ deceleration and constant speed sections.

During the first 405.494 ms, the armature moves forwards up to 483.246 mm, providing a 48-N machining force at 25 m/min between 284.257 and 384.257 ms —see Figs. 4(a) and 2(b). Then, the motor returns immediately to the initial position in 322.617 ms, and remains at a standstill

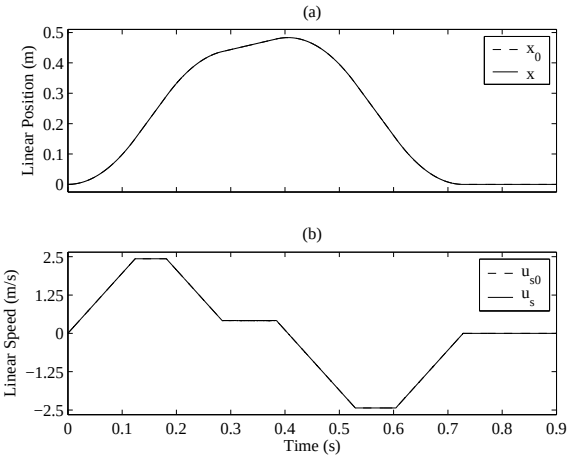

Fig. 2. Linear position and speed responses

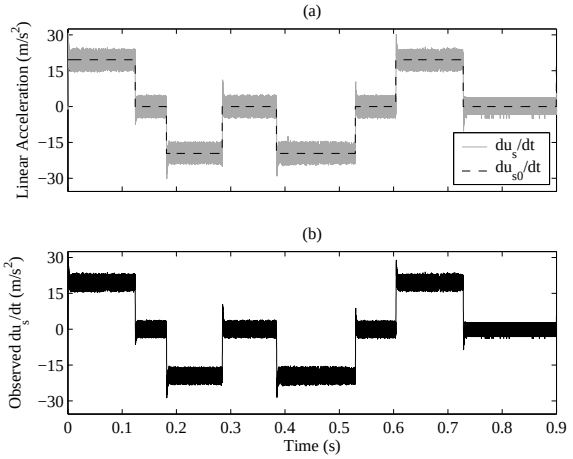

Fig. 3. Reference, actual and observed linear accelerations

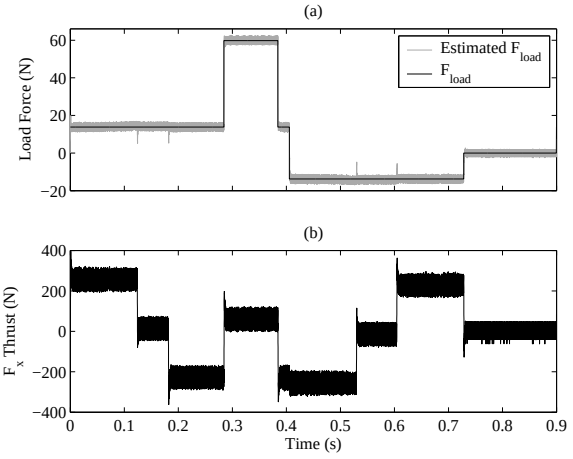

Fig. 4. Actual and observed load force, and motor thrust

for 171.678 ms to conclude the cycle. Maximum traversing speeds of 143 m/min are reached.

It should be noted that, in addition to the above-mentioned machining force, F_{load} comprises also a 13.8-N force caused by Coulomb's friction, which obstructs motion in both directions. Motor thrust

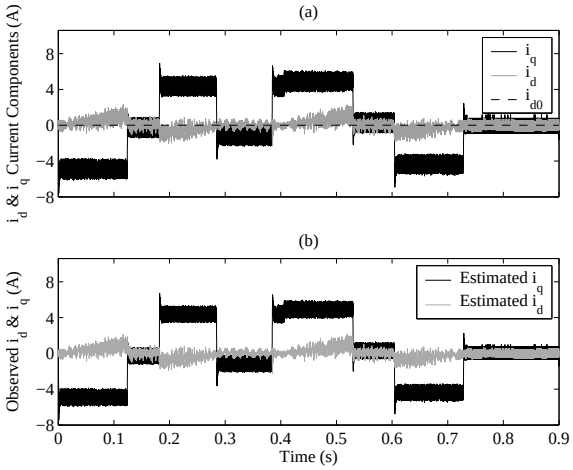

Fig. 5. Actual and estimated armature current components

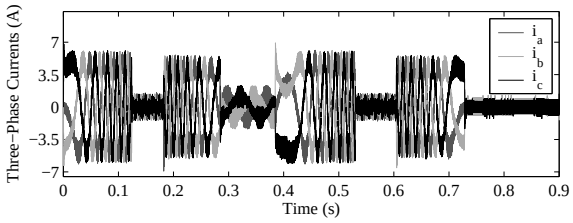

Fig. 6. Three-phase armature currents

in Fig. 4(b) compensates the load force and provides the acceleration/deceleration required to achieve satisfactory tracking.

Performances of the load force and current observers can be examined in Figs. 4(a) and 5. Based on such estimates, the linear acceleration in Fig. 3(b) has been derived as indicated by (35) and (36). Note that reference value i_{d0}, displayed in Fig. 5(a), is kept equal to zero during the whole cycle. Below the rated speed, completion of this condition leads LPMSM's with surface-mounted magnets to provide maximum thrust per current unit (Vas, 1998). As a result, motor thrust variations observed in Fig. 4(b) are directly related to changes in i_q. Fig. 6 reflects the three-phase armature currents corresponding to the i_d and i_q components shown in Fig. 5(a).

To conclude, the dynamic performance of switching variables s_1, s_2 and s_3 around zero is presented in Fig. 7.

5. CONCLUSIONS

To a certain extent, the servo positioning system discussed in this paper may be viewed as general-purpose, since it is applicable to LPMSM's with either interior or surface-mounted magnets, no matter which element —armature or magnets— is movable and which stationary.

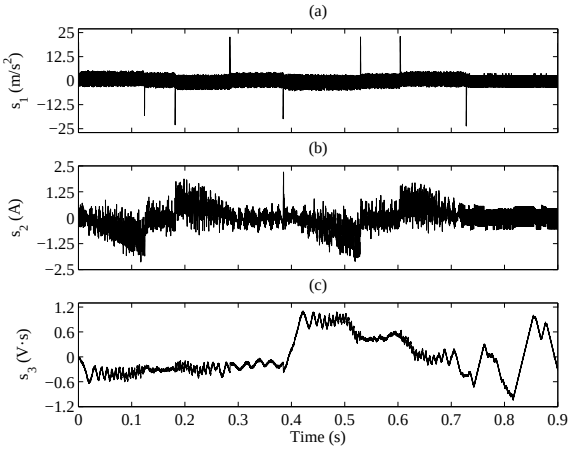

Fig. 7. Time progress of the switching variables

So far, simulation results obtained for different reference trajectories and load cycles reveal that sliding-mode control provides the LPMSM under consideration with an outstanding ability for linear position tracking. It has also been verified that considerable variations on both the total mass shifted and viscous friction do not affect the tracking performance substantially, even though neither the sliding-mode controller nor the load force observer are re-tuned.

As expected, the continuous-time framework assumed for controller design leads to discretization chatter, which augments appreciably as the sample rate decreases. However, although the increase of discretization chatter caused by sample rate reduction becomes apparent in current, thrust and acceleration waveforms, it is not that significant in speed, and even much less in position.

ACKNOWLEDGEMENTS

This work is supported by the research program of the Spanish Science and Technology Ministry (MCYT).

REFERENCES

Boldea, I. and S.A. Nasar (2001). *Linear Motion Electromagnetic Devices*. Taylor & Francis. USA.

Bondarev, A.G., S.A. Bondarev, N.E. Kostyleva and V.I. Utkin (1985). Sliding modes in systems with asymptotic state observers. *Automation and Remote Control* **46**(6), 49–64.

Gieras, J.F. and Z.J. Piech (2000). *Linear Synchronous Motors: Transportation and Automation Systems*. CRC Press LLC, 2000 N.W. Corporate Blvd.. Boca Raton, Florida, USA.

SIEMENS AG (1999–2002). SIMODRIVE Linear Motors 1FN1 and 1FN3 (PJLM) – 06.02 Edition, ALL-45–49.

Renton, D. and M.A. Elbestawi (2001). Motion control for linear motor feed drives in advanced machine tools. *Int. Journal of Machine Tools & Manufacture* **41**(4), 479–507.

Utkin, V., J. Guldner and J. Shi (1999). *Sliding Mode Control in Electromechanical Systems*. Taylor & Francis. Padstow, UK.

Utkin, V.I. (1993). Sliding mode control design principles and applications to electric drives. *IEEE Transactions on Industrial Electronics* **40**(1), 23–36.

Vas, P. (1996). *Electrical Machines and Drives: A Space-Vector Theory Approach*. Clarendon Press Oxford. New York.

Vas, P. (1998). *Sensorless Vector and Direct Torque Control*. Oxford University Press. New York.

Weidner, C. and D. Quickel (1999). High-speed machining with linear motors. *Manufacturing Engineering* **122**(3), 80–90.

Appendix A

Table A.1. Characteristic parameters of LPMSM 1FN3 050-2WC00-0AA0 by SIEMENS.

Parameter	Value	Description
R_s	13.9 Ω	Armature resistance per phase at 120 °C
L_d	0.0365 H	d-axis armature inductance per phase
L_q	0.0365 H	q-axis armature inductance per phase
λ_{PM}	0.0238 Wb	Flux of the permanent magnets
τ	0.015 m	Pole pitch
P	7	Number of pole pairs
k	-1	Movable armature and stationary magnets
$I_{peak\,max}$	$8.2\sqrt{2}$ A	Peak value of the maximum admissible current
$F_{x\,max}$	550 N	Maximum thrust the motor is able to provide
$F_{x\,N}$	200 N	Nominal motor thrust
$u_{s\,rated}$	143 m/min	Rated linear speed at maximum thrust
M	12.45 kg	Total mass —armature plus load— shifted
f	negligible	Viscous friction coefficient

Table A.2. Parameters related to the Sliding-Mode Control algorithm.

Parameter	Value	Description
ξ	1	Damping factor of the position error vanishing dynamics in sliding regime
ω_n	580 rad/s	Natural frequency of the position error vanishing dynamics in sliding regime
U_d	600 V	DC-link voltage
ℓ	28884 kg/s	Gain of the linear load force observer
f_s	23.2 kHz	Sample rate